# Nanoparticle Targeting of Anticancer Drug Improves Therapeutic Response in Animal Model of Human Epithelial Cancer

Jolanta F. Kukowska-Latallo,[1] Kimberly A. Candido,[1] Zhengyi Cao,[1] Shraddha S. Nigavekar,[2] Istvan J. Majoros,[1] Thommey P. Thomas,[1] Lajos P. Balogh,[1] Mohamed K. Khan,[2] and James R. Baker, Jr.[1]

[1]University of Michigan Center for Biologic Nanotechnology and [2]Department of Radiation Oncology, University of Michigan Health System, Ann Arbor, Michigan

## Abstract

Prior studies suggested that nanoparticle drug delivery might improve the therapeutic response to anticancer drugs and allow the simultaneous monitoring of drug uptake by tumors. We employed modified PAMAM dendritic polymers <5 nm in diameter as carriers. Acetylated dendrimers were conjugated to folic acid as a targeting agent and then coupled to either methotrexate or tritium and either fluorescein or 6-carboxytetramethylrhodamine. These conjugates were injected i.v. into immunodeficient mice bearing human KB tumors that overexpress the folic acid receptor. In contrast to nontargeted polymer, folate-conjugated nanoparticles concentrated in the tumor and liver tissue over 4 days after administration. The tumor tissue localization of the folate-targeted polymer could be attenuated by prior i.v. injection of free folic acid. Confocal microscopy confirmed the internalization of the drug conjugates into the tumor cells. Targeting methotrexate increased its antitumor activity and markedly decreased its toxicity, allowing therapeutic responses not possible with a free drug. (Cancer Res 2005; 65(12): 5317-24 )

## Introduction

The high-affinity folate receptor for the vitamin folic acid, also known as the folate-binding protein, has been used as a target for the delivery of folate-conjugated drugs to cancer tissue (1). The folate receptor is overexpressed in breast, ovary, endometrium, kidney, lung, head and neck, brain, and myeloid cancers (2–5) and is internalized into cells after ligand binding (6). Tumor-selective targeting has been achieved by combining folic acid–conjugated liposomes with antineoplastic drugs (7) or antisense oligonucleotides (8), folate-conjugated protein toxins (9), and folic acid–derivatized antibodies or their Fab/scFv fragments binding to the T-cell receptor (10). Direct conjugation of drugs or other molecules to folic acid, however, can lead to reduced folate binding or to alteration of the function of the therapeutic moiety (11). In addition, the affinity of folate conjugates is limited when coupling only a single folate molecule to a drug (12). It would also be desirable to combine imaging with targeted therapy as a measure of drug delivery, but this would require a delivery by a single targeting moiety.

Polyamidoamine dendrimers are well-characterized, highly branched synthetic macromolecules that are biocompatible and nonimmunogenic, providing a unique platform for delivery of a variety of therapeutic agents, imaging agents, and oligonucleotides (13–19). We have reported previously the synthesis of folic acid–conjugated, surface-modified PAMAM dendrimers and have shown in vitro the highly selective binding and internalization of these polymers in tumor cells that overexpress folate receptor (20). It also appeared that there was cooperative binding between multiple folic acid molecules on the surface of the polymer and multiple folate receptor on the membranes of tumor cells leading to higher avidity interactions.

Prior studies from our group and others have shown that, when injected into the vascular system in mice, nontargeted PAMAM dendrimers distribute according to size with similar characteristics to proteins of the same molecular weight (13). In addition, neutralization of the amine surface charge of the dendrimer is essential to preventing toxicity and nonspecific uptake of the drug conjugates (20, 21). In the current studies, we therefore sought to evaluate the ability of folic acid–targeted, surface-modified dendrimers to serve as a platform for the targeted delivery of anticancer therapeutics and imaging agents to xenograft human KB tumors in mice. We examined the biodistribution, imaging potential, and antitumor efficacy of folic acid–targeted dendrimers covalently coupled to methotrexate, radionuclides, and fluorescent dyes and compared this with free drug and nontargeted polymer controls. The results suggest the potential utility of these conjugates for medical applications.

## Materials and Methods

**Materials and reagents.** All reagents were obtained from commercial sources. Folic acid, penicillin/streptomycin, fetal bovine serum, collagenase type IV, TX100, bis-benzimide, FITC, methotrexate, hydrogen peroxide, acetic anhydride, ethylenediamine, methanol, dimethylformamide, and DMSO were purchased from Sigma-Aldrich (St. Louis, MO). Trypsin-EDTA, Dulbecco's PBS, and RPMI 1640 (with or without folic acid) were from Invitrogen (Gaithersburg, MD). "Solvable" solution and hionic fluor were from Packard Bioscience (Downers Grove, IL). OCT embedding medium was from Electron Microscopy Sciences (Fort Washington, PA), 2-methyl butane from Fisher Scientific (Pittsburgh, PA), and 6-carboxytetramethylrhodamine (6-TAMRA) and Prolong were from Molecular Probes, Inc. (Eugene, OR). Tritium-labeled acetic anhydride $(CH_3CO)_2O$ [$^3H$] (100 mCi, 3.7 GBq) was purchased from ICN Biomedicals (Irvine, CA). Methotrexate for injection was from Bedford Laboratories (Bedford, OH). Folic acid was solubilized in saline, adjusted to pH 7.0 with 1 N NaOH, and filter sterilized for injections.

**Synthesis and characterization of PAMAM dendrimer conjugates.** A G5 PAMAM dendrimer was synthesized and purified from low molar mass contaminants as well as higher molar mass dimers or oligomers (22). The number average molar mass of the dendrimer was determined to be

26,530 g/mol by size exclusion chromatography using multiangle laser light scattering, UV, and refractive index detectors. The average number of surface primary amine groups in the dendrimer was determined to be 110 using potentiometric titration along with the molar mass. The polydispersity index, defined as the ratio of weight average molar mass and number average molar mass for an ideal monodisperse sample, equals 1.0. The polydispersity index of G5 dendrimer was calculated to be 1.032, indicating very narrow distribution around the mean value and confirming the high purity of the G5 dendrimer. The surface amines of G5 PAMAM dendrimers were acetylated with acetic anhydride to reduce nonspecific binding of the dendrimer. The ratio between the acetic anhydride and the dendrimer was selected to achieve different acetylation levels from 50 to 80 and 100 primary amines. After purification, the acetylated dendrimer was conjugated to either FITC or 6-TAMRA as the label for detection and imaging. The dye-conjugated dendrimer was then allowed to react with an activated ester of folic acid, and the purified product of this reaction was analyzed by $^1$H nuclear magnetic resonance (NMR) to determine the number of conjugated folic acid molecules. Subsequently, methotrexate was conjugated via ester bond as described previously (20).

Radiolabeled compounds were synthesized from G5-(Ac)$_{50}$-(FA)$_6$ or G5-(Ac)$_{50}$ using tritiated acetic anhydride (Ac-$^3$H) as described previously (18, 21, 23). The tritiated conjugates, G5-$^3$H-FA and G5-$^3$H, were fully acetylated. The specific activity of the G5-NHCOC-$^3$H and G5-FA-NHCOC-$^3$H conjugates were 10.27 and 38.63 mCi/g, respectively. The residual free tritium was <0.3% of the total activity.

The quality of the PAMAM dendrimer conjugates was tested using PAGE, $^1$H NMR, $^{13}$C NMR, and mass spectroscopy. Capillary electrophoresis was used to confirm the purity and homogeneity of the final products.

The folic acid–targeted conjugates specifically contain the following molecules: G5-(Ac)$_{82}$-(FITC)$_5$-(FA)$_5$, G5-(Ac)$_{82}$-(6-TAMRA)$_3$-(FA)$_4$, G5-(Ac)$_{82}$-(FITC)$_5$-(FA)$_5$-MTX$_5$, and G5-(Ac)$_{50}$-(Ac-$^3$H)$_{54}$-(FA)$_6$, which were identified with the acronyms G5-FI-FA, G5-6T-FA, G5-FI-FA-MTX, and G5-$^3$H-FA, respectively. The nontargeted controls contained the following molecules: G5-(Ac)$_{82}$-(FITC)$_5$, G5-(Ac)$_{82}$-(6-TAMRA)$_3$, G5-(Ac)$_{82}$-(FITC)$_5$-MTX$_5$, and G5-(Ac)$_{50}$-(Ac-$^3$H)$_{54}$, which were identified with the acronyms G5-FI, G5-6T, G5-FI-MTX, and G5-$^3$H, respectively.

**Recipient animal and tumor model.** Immunodeficient, 6- to 8-week-old athymic nude female mice [Sim:(NCr) *nu/nu* fisol] were purchased from Simonsen Laboratories, Inc. (Gilroy, CA). Five- to 6-week-old Fox Chase severe combined immunodeficient (SCID; CB-17/lcrCrl-scidBR) female mice were purchased from the Charles River Laboratories (Wilmington, MA) and housed in a specific pathogen-free animal facility at the University of Michigan Medical Center in accordance with the regulations of the University's Committee on the Use and Care of Animals as well as with federal guidelines, including the Principles of Laboratory Animal Care. Animals were fed *ad libitum* with Laboratory Autoclavable Rodent Diet 5010 (PMI Nutrition International, St. Louis, MO). Three weeks before tumor cell injection, the food was changed to a folate-deficient diet (TestDiet, Richmond, IN). For urine and feces collection, animals were housed in metabolic rodent cages (Nalgene, Rochester, NY).

**Tumor cell line.** The KB human cell line, which overexpresses the folate receptor (24), was purchased from the American Type Tissue Collection (Manassas, VA) and maintained *in vitro* at $37°C$, 5% $CO_2$ in folate-deficient RPMI 1640 supplemented with penicillin (100 units/mL), streptomycin (100 μg/mL), and 10% heat-inactivated fetal bovine serum. Before injection in the mice, the cells were harvested with trypsin-EDTA solution, washed, and resuspended in PBS. The cell suspension ($5 \times 10^6$ cells in 0.2 mL) was injected s.c. into one flank of each mouse using a 30-gauge needle. In the biodistribution studies, the tumors were allowed to grow for 2 weeks until reaching ∼0.9 cm$^3$ in volume. The formula chosen to compute tumor volume was for a standard volume of an ellipsoid, where $V = 4/3\pi$ (1/2 length × 1/2 width × 1/2 depth). With an assumption that width equals depth and π equals 3, the formula used was $V = 1/2 \times$ length × width$^2$. Targeted drug delivery using conjugate injections was started on the fourth day after implantation of the KB cells.

**Biodistribution and excretion of tritiated dendrimer.** Animals were injected via lateral tail vein with 0.5 mL PBS solution containing 174 μg G5-NHCOC-$^3$H (1.8 μCi) or 200 μg G5-FA-NHCOC-$^3$H (7.7 μCi). Both tritium-labeled conjugates were delivered at equimolar concentrations of the modified dendrimer. At 5 minutes, 2 hours, 1 day, 4 days, and 7 days postinjection, the animals were euthanized and samples of tumor, heart, lung, liver, spleen, pancreas, kidney, and brain were taken. A third group of mice received a bolus of 80 μg free folic acid 5 minutes before injection with 200 μg G5-$^3$H-FA. This 181 nmol concentration of free folic acid yields ∼150 μmol/L concentration in the blood compared with radiolabeled targeted dendrimer (G5-$^3$H-FA), which yields ∼5 μmol/L concentration in the blood and is based on the 1.2 mL blood volume of a 20 g mouse. The mice were euthanized at 5 minutes, 1 day, and 4 days following injection, and tissues were harvested as above. Blood was collected at each time point via cardiac puncture. Each group included three to five mice. Urine and feces samples were collected at 2, 4, 8 and 12 hours and 1, 2, 3, and 4 days.

Radioactive tissue samples were prepared exactly as described previously (21). The tritium content was measured in a liquid scintillation counter (LS 6500, Beckman Coulter, Fullerton, CA). The values of measured radioactivity were adjusted for the counting efficiency of the instrument and used to derive radioactivity (1 μCi = $2.22 \times 10^6$ dpm) per sample. These values were then normalized by tissue weight and the specific radioactivity of the conjugates was reported as a percentage of the injected dosage (% ID/g). The excreted radioactivity (dendrimer) via urine and feces was reported as a percentage of the injected dosage (% ID).

**Biodistribution of fluorescent dendrimer conjugates.** Mice were injected via lateral tail vein with 0.5 mL saline solution containing 0.2 mg of G5-6T or G5-6T-FA conjugates. At 15 hours and up to 4 days postinjection, the animals were euthanized and samples of tumor were taken and immediately frozen for sectioning and imaging.

Flow cytometry analysis was done with single-cell suspension isolated from tumor. Tumor was crushed, cell suspension filtered through 70 μm nylon mesh (Becton Dickinson, Franklin Lakes, NJ), and washed with PBS. Samples were analyzed using an EPICS XL flow cytometer (Coulter, Miami, FL). As determined by prior propidium iodine staining, only live cells were gated for analysis. Data were reported as the mean channel fluorescence of the cell population.

For confocal microscope imaging, tissue was dissected, embedded in OCT, and frozen in 2-methyl-butane in a dry ice bath. Sections (15 μm) were cut on a cryostat, thaw mounted onto slides, and stored at $-80°C$ until stained. After staining, the slides were fixed in 4% paraformaldehyde, rinsed in phosphate buffer (0.1 mol/L; pH 7.2), and mounted in Prolong. The images were acquired using a Zeiss 510 metalaser scanning confocal microscope equipped with a ×40 Plan-Apo 1.2 numerical aperture (water immersion) objective with a correction collar. The confocal image was recorded as $512 \times 512 \times 48$ pixels with a scale of $0.45 \times 0.45 \times 0.37$ μm per pixel. Each image cube was optically cut into 48 sections, and the sections that cut through the nucleus and cytoplasm were presented.

**Delivery of targeted nanoparticle therapeutic.** Twice weekly, SCID mice with s.c. KB xenografts, starting on day 4 after tumor implantation, received via the tail vein an injection of either targeted or nontargeted conjugate containing methotrexate, a conjugate without methotrexate, free methotrexate, or saline as a control. The compounds were delivered in a 0.2 mL volume of saline per 20 g of mouse. The single dose of methotrexate delivered each time equaled 0.33 mg/kg. The higher doses of 1.67 and 3.33 mg/kg free methotrexate were also tested. The conjugates were delivered at equimolar concentration of methotrexate calculated based on the number of methotrexate molecules present in a nanoparticle. The conjugate without methotrexate was delivered at equimolar concentration of dendrimer. In the initial trial, six groups of mice with five mice in each group received up to 15 injections. In the follow-up trial, mice received up to 28 injections dependent on their survival. The body weights of the mice were monitored throughout the experiment as an indication of adverse effects of the drug. Histopathology of multiple organs was done at the termination of each trial and each time mouse had to be euthanized due to toxic effects or tumor burden. Tissues from lung, heart, liver, pancreas, spleen, kidney, and tumor were analyzed. Additionally, cells were isolated from tumors, stained with targeted fluorescein-labeled conjugate, and tested for the presence of folic acid receptors using flow cytometer.

**Statistical methods.** Means, SD, and SE of the data were calculated. Differences between the experimental groups and the control groups were tested using Student's-Newman-Keuls' test and $P$s < 0.05 were considered significant.

## Results

**Synthesis of conjugated dendrimer nanoparticles.** The PAMAM G5 dendrimer was synthesized, purified, and characterized in the Center for Biologic Nanotechnology at the University of Michigan as described in Materials and Methods. To prevent nonspecific biological interactions of charged surface amino groups, 70% to 90% of the primary amines were acetylated in drug conjugate or radiolabeled conjugate, respectively (13, 20). Four pairs of nanoparticles were synthesized, with both members of each pair containing the same tracer. One member of each pair contained FA- one pair with, one pair without the antineoplastic drug MTX-, whereas the other conjugate lacked folic acid and served as a nontargeted control with or without the drug. The exact content of each pair of molecules is listed in Materials and Methods.

**Biodistribution of tritiated dendrimers.** We first examined the biodistribution and elimination of tritiated G5-$^3$H-FA to test its ability to target the folate receptor–positive human KB tumor xenografts established in immunodeficient nude mice. The mice were maintained on a folate-deficient diet for the duration of the experiment to minimize the circulating levels of folic acid (25). The free folic acid level achieved in the serum of the mice before the experiment approximated human serum levels (26, 27). Mice were evaluated at various time points (5 minutes to 7 days) following i.v. administration of the conjugates. Two groups of mice received either control nontargeted tritiated G5-$^3$H dendrimer or targeted tritiated G5-$^3$H-FA conjugate (Fig. 1$A$ and $B$).

The conjugates were cleared rapidly from the blood via the kidneys during the first day postinjection, with the G5-$^3$H decreasing from 23.4% ID/g tissue at 5 minutes to 1.8% ID/g at 1 day (Fig. 1$A$). The blood concentration of G5-$^3$H-FA decreased from 29.1% ID/g at 5 minutes to 0.2% ID/g at 1 day (Fig. 1$B$). In several organs, such as the lung, the tissue distribution showed a trend similar to blood concentrations with G5-$^3$H decreasing from 9.7% ID/g at 5 minutes to 1.6% ID/g at 1 day and G5-$^3$H-FA decreasing from 9.6% ID/g at 5 minutes to 1.7% ID/g at 1 day. Due to the high vascularity of the lung, conjugate levels measured at early time points likely reflect blood concentrations. Similar patterns of clearance were observed for the heart, pancreas, and spleen. These organs are known not to express folate receptor and do not show significant differences between the nontargeted and the targeted dendrimers. The concentrations of both G5-$^3$H and G5-$^3$H-FA in the brain were low at all time points, suggesting that the polymer conjugates did not cross the blood-brain barrier (Fig. 1$A$ and $B$). Although the kidney is the major clearance organ for these dendrimers, it is also known to express high levels of the folate receptor on its tubules. The level of nontargeted G5-$^3$H in the kidney decreased rapidly and was maintained at a moderate level over the next several days (Fig. 1$A$). In contrast, the level of G5-$^3$H-FA increased slightly over the first day most likely due to folate receptor present on the kidney tubules. This was followed by a decrease over the next several days as the compound was cleared through the kidney (Fig. 1$B$).

Both G5-$^3$H and G5-$^3$H-FA were rapidly excreted, primarily through the kidney, within 24 hours following injection (data not shown). Incremental excretion of both compounds appeared

entirely consistent with kidney retention of the conjugates (Fig. 1$A$ and $B$). Although both targeted and nontargeted conjugates also appeared in feces, it was in very low amounts. Whether any material was actually excreted in the feces was difficult to determine due to minor urine contamination of the feces. The cumulative clearance of the targeted G5-$^3$H-FA over the first 4 days was lower than that of G5-$^3$H, which may reflect retention of G5-$^3$H-FA within tissues expressing folate receptors.

The liver and KB tumor cells are known to express high levels of folate receptor. In these tissues, the concentrations of nontargeted G5-$^3$H decreased rapidly with clearance of the dendrimer from the blood; the concentrations were maintained at a low level over the remaining days that the tissues were studied (Fig. 1$A$). In contrast, in both the liver and tumor, the targeted G5-$^3$H-FA content increases over the first 4 days (Fig. 1$B$). This occurs during a time when blood levels of radioactive conjugate are low, suggesting specific uptake against a concentration gradient of dendrimer in these tissues, as opposed to the simple trapping of dendrimer through the vasculature.

The specificity of targeted drug delivery was further addressed in a group of mice receiving 181 nmol free folic acid before injection with G5-$^3$H-FA (Fig. 1$C$). At 4 days after injection, significant attenuation in radioactivity related to the blocking of folate receptor with free folic acid was observed in tumor tissue that does not have the ability to excrete the dendrimer (Fig. 1$C$). This suggests that the difference in tumor concentrations between the targeted and the nontargeted polymer conjugates is due to the specific uptake of these molecules through the folate receptor overexpressed in the tumor. Distribution in all other tissues was not significantly altered by the delivery of free folic acid before the injection of the targeted conjugate (data not shown).

**Targeting and internalization of fluorescent dendrimer conjugate.** To further confirm and localize the dendrimer nanoparticles within tumor tissue, dendrimers conjugated with 6-TAMRA were employed. Confocal microscopy images were obtained of tumor samples at 15 hours following i.v. injection of the targeted G5-6T-FA and the nontargeted G5-6T conjugates (Fig. 2$A$-$C$). The tumor tissue showed a significant number of fluorescent cells with targeted dye-conjugated dendrimer G5-6T-FA (Fig. 2$B$) compared with those with nontargeted dendrimer (Fig. 2$A$). Flow cytometry analysis of a single-cell suspension isolated from the same tumors showed higher mean channel fluorescence for tumor cells from mice receiving G5-6T-FA (Fig. 2$C$). Previously, we have obtained similar results while demonstrating targeting to tumor cells using a two-photon optical fiber probe for the detection of fluorescence (28).

Confocal microscopy also showed that at 4 days the conjugate is present in the tumors, attached to and internalized by many of the tumor cells (Fig. 2$D$). The optical overlapping sections were taken of the tissue slides from apical through medial to basal section. The medial section of tumor cells presented herein show fluorescence throughout the cytosol from the 6T of the conjugate, with the cell and nucleus boundary clearly visible (Fig. 2$D$).

**Toxicity of dendrimer conjugates.** All mice were observed for the duration of the studies for signs of dehydration, inability to eat or drink, weakness, or change in activity level. No gross toxicity, either acutely or chronically up to 99 days, was observed regardless of whether the dendrimer conjugate contained methotrexate. The weight was monitored throughout the experiment and no loss of weight was observed; in fact, the animals gained weight. At each time point, a gross examination and histopathology of the liver,

spleen, kidney, lung, and heart were done. No morphologic abnormalities were observed on the histopathology examination. No *in vivo* toxicity was noted in any animal group following the dendrimer injection.

**Targeted drug delivery to tumor cells through the folate receptor.** The efficacy of different doses of conjugates was tested on SCID CB-17 mice bearing s.c. human KB xenografts and was compared with equivalent and higher doses of free methotrexate.
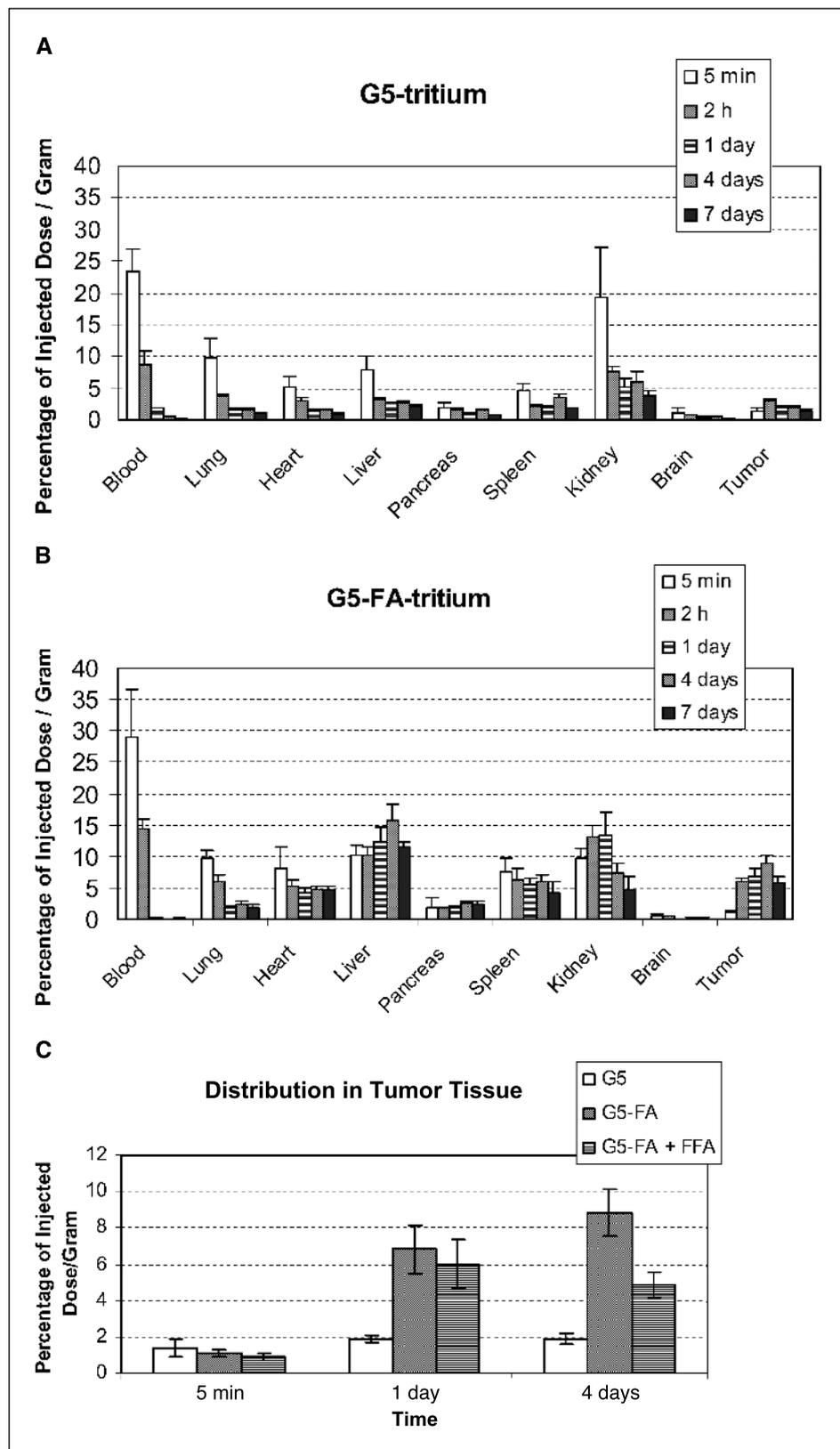


**Figure 1.** Biodistribution of radiolabeled nontargeted (*A*) and targeted (*B*) conjugate in *nu/nu* mice bearing KB xenograft tumor depicted as percentage of injected dose of dendrimer recovered per gram of organ. *Columns,* mean for different organs at 5 minutes, 2 hours, and 1, 4, and 7 days after delivery of (*n* = 3-5 mice); *bars,* SD. *C,* inhibition of distribution of targeted conjugate in tumor after preinjection of mice with 181 nmol free folic acid (*FFA*) is compared with the distribution of nontargeted and targeted conjugate at 5 minutes, 1 day, and 4 days. Inhibition is significantly lower at 4 days (at least *P* < 0.05).
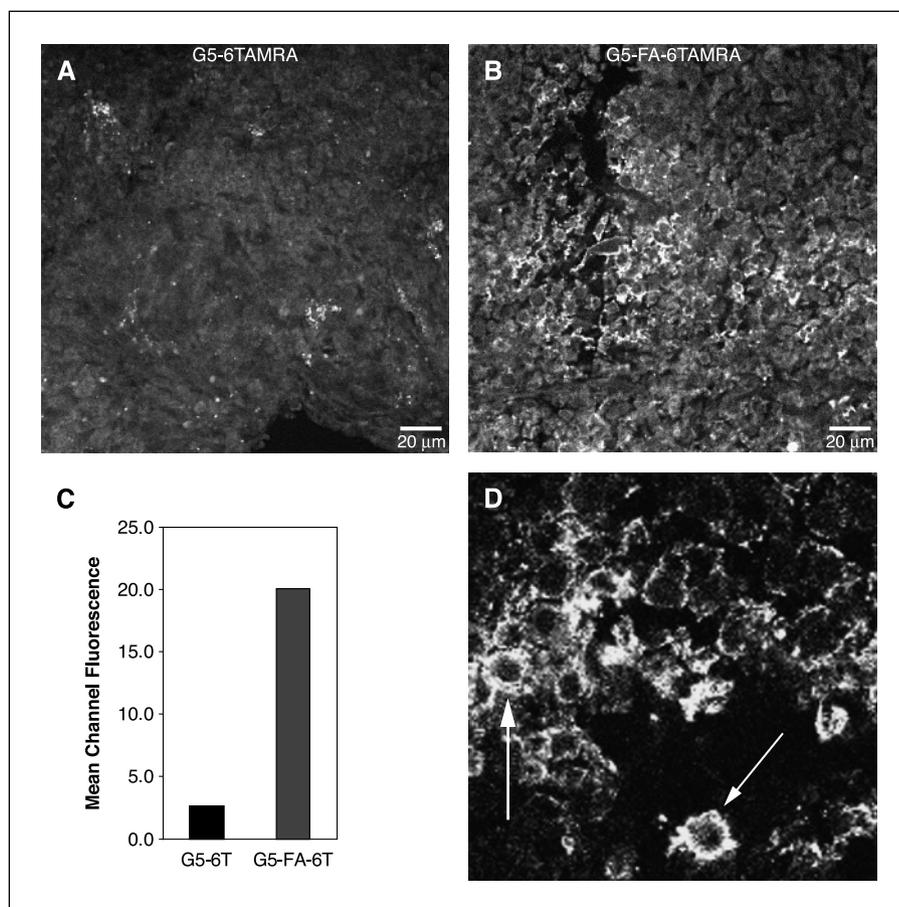
**Figure 2.** Confocal microscopy analysis of cryosectioned tumor samples from SCID mice that were injected with 10 nmol of either nontargeted G5-6-TAMRA (*A*) or targeted G5-FA-6-TAMRA conjugate 15 hours (*B*) or 4 days (*D*) before tumor isolation. Flow cytometry analysis done on the isolated cells from the same tumor (*B*) concur that tumor cells specifically uptake G5-FA-6-TAMRA compared with G5-6-TAMRA (*C*). The enlargement shows the cells in the medial optical section with significant fluorescence of 6-TAMRA attached to the targeted conjugate (*D*). *Arrows,* clearly visible cytoplasm around the nucleus.

Mice were maintained on the folic acid–deficient diet for 3 weeks before injection of the KB tumor cells to achieve circulating levels of folic acid that approach those in human serum and to prevent down-regulation of folate receptors on tumor xenografts (25). Six groups of SCID mice with five mice in each group were injected s.c. on one flank with $5 \times 10^6$ KB cells in 0.2 mL PBS suspension. The highest total dose of G5-FI-FA-MTX therapeutic used equals 55.0 mg/kg and is equivalent to a 5.0 mg/kg total cumulative dose of free methotrexate (Fig. 3). The therapeutic dose of the conjugate was compared with three cumulative doses of free methotrexate equivalent to 33.3, 21.7, and 5.0 mg/kg accumulated in 10 to 15 injections based on mouse survival. Saline and the conjugate without methotrexate (G5-FI-FA) were used as controls. The body weights of the mice were monitored throughout the experiment as an indication of adverse effects of the drug, and the changes of body weight showed acute and chronic toxicity in the highest and in the second highest cumulative doses of free methotrexate equal to 33.3 and 21.7 mg/kg, respectively (data not shown). Although the two doses of free drug were affecting tumor growth, both became lethal by days 32 to 36 of the trial (Fig. 3). The remaining experimental groups had very uniform body weight fluctuations nonindicative of toxicity when compared with control groups with saline or conjugate without methotrexate (data not shown). For the highest cumulative doses of free methotrexate used, histopathology analysis of the liver revealed advanced liver lesions, collections of inflammatory cells, and periportal inflammation (data not shown). In contrast, neither the total accumulated dose of therapeutic conjugate equivalent to 5.0 mg/kg of free methotrexate nor free

methotrexate at the same dose were toxic (Fig. 3). Importantly, the therapeutic dose of conjugate that was equal to the lowest dose of free methotrexate used was as equally effective as the second highest dose of free methotrexate (21.7 mg/kg in 13 injections), whereas the free drug at this concentration had no effect on tumor growth (Fig. 3). The conjugate without methotrexate (G5-FI-FA) also had no therapeutic effect when compared with control injections of saline (Fig. 3). The liver slides from mice receiving the conjugate (G5-FI-FA-MTX) showed occasional periportal lympho-cytes, indicating inflammation and single-cell necrosis that did not differ from that of control animals injected with saline (data not shown).

During a second 99-day trial, there was a statistically significant ($P < 0.05$) slower growth of tumors that were treated with G5-FI-FA-MTX or G5-FA-MTX conjugate without FITC compared with those treated with nontargeted G5-FI-MTX conjugate, free methotrexate, or saline. The equivalent dose of methotrexate delivered with both targeted conjugates to the surviving mice was higher than the dose of free methotrexate because all of the mice receiving free methotrexate died by day 66 of the trial (Fig. 4). The survival of mice from groups receiving G5-FI-FA-MTX or G5-FA-MTX conjugate indicate that tumor growth based on the end-point volume of 4 cm$^3$ can be delayed by at least 30 days (Fig. 4). This value indicates the antitumor effectiveness of the conjugate because it mimics clinical end-points and requires observation of the mice throughout the progression of the disease. We have achieved a complete cure in one mouse treated with G5-FA-MTX conjugate at day 39 of the trial. The tumor in this mouse was not

palpable for the next 20 days up to the 60th day of the trial. At the termination of the trial, there were three (of eight) survivors receiving G5-FA-MTX and two (of eight) survivors receiving G5-FI-FA-MTX. There were no mice surviving in the group receiving free methotrexate or in any other control group. The effective dose of conjugate was not toxic based on weight change and the histopathology examination that was done (data not shown).

At the termination of both trials, histopathology examination did not reveal signs of toxicity in the heart and myopathy did not develop. We did not observe acute tubular necrosis in the kidneys of these animals. Analysis of tumor slides showed viable tumors with mild necrosis in the control and saline-injected animals, whereas the therapeutic conjugate caused severe to significant necrosis in tumors compared with an equivalent dose of free methotrexate (data not shown). At the termination of the trial, tumor cells were evaluated for possible up-regulation of folic acid receptor in tumor compared with KB cells due to a long-term folic acid–depleted diet of mice. Flow cytometry analysis of tumor cells after staining with targeted fluorescein-labeled conjugate revealed that cells remained folic acid receptor positive but at two to five times lower level compared with original KB cell line (data not shown).

## Discussion

Current cancer chemotherapies are dose limited by side effects resulting from cytotoxicity that kills normal as well as tumor cells. Although some newer cancer drugs target unique metabolic aspects of cancers (29), many cancers do not have this type of specific metabolic target. Another approach to targeted cancer therapy aims to reduce or eliminate side effects by delivering a cytotoxic pharmaceutical to specific cells (1). However, this approach has been limited by the absence of high-affinity targeting ligands with relative specificity for cancer cells and by the limitation on size of the targeted material (<50 nm) required to escape the vasculature and to interact with the individual tumor cells. Antibodies have been used for targeting therapeutics with success, but problems with immunogenicity and retention in the reticuloendothelial system remain (30, 31). Larger molecules like liposomes may extravasate to reach tumor cells to some degree but have primarily been used to target tumor vasculature (32, 33). Other approaches have attempted to target tumors through the enhanced permeability of their blood vessels, but this appears to work mainly in larger tumors (34). Therefore, having a targeting therapeutic that is small enough to reach tumor cells and internalize with specificity is desirable.

Dendrimer-based drug delivery molecules have several potential advantages. Dendrimers are comparable in size to proteins, being small enough (<5.0 nm diameter) to escape the vasculature and target tumor cells while also being below the threshold of renal filtration to allow urinary excretion. This latter asset avoids retention in filter organs and therefore removes a requirement for hepatic metabolism. The G5 PAMAM dendrimer is stable, non-immunogenic, and contains, on average, 110 to 128 primary amines on the surface. This provides ample reactive sites for the conjugation of complex drug delivery systems and multiple chemical moieties, such as radiopharmaceuticals, dyes, and contrast agents. Dendrimers also can be chemically synthesized in large quantities as monodispersed populations, allowing for potential scale-up of the technology.

This report documents for the first time tumor cell–targeted delivery and therapeutic effect of drug-dendrimer conjugates *in vivo*. The levels of targeted radiolabeled conjugates in the liver, kidney, and tumor, tissues that express high levels of the folate receptor, increased over the first 4 days in contrast to the concentrations of nontargeting dendrimer, which dropped significantly in these tissues within 2 hours after injection (Fig. 1*A* and *B*). Uptake of the targeted but not the control dendrimer in the tumor could be partially inhibited by prior administration of excess of free folic acid (Fig. 1*C*). Excretion of both molecules was rapid and occurred primarily through the kidney; however, a larger percentage of the nontargeted material was excreted at all time points. The differences in accumulation, distribution, and excretion of the folate-targeted and nontargeted radioactive dendrimers suggest that there is preferential uptake based on the presence of folic acid receptors on the cell membranes of these tissues (Fig. 1*A-C*).
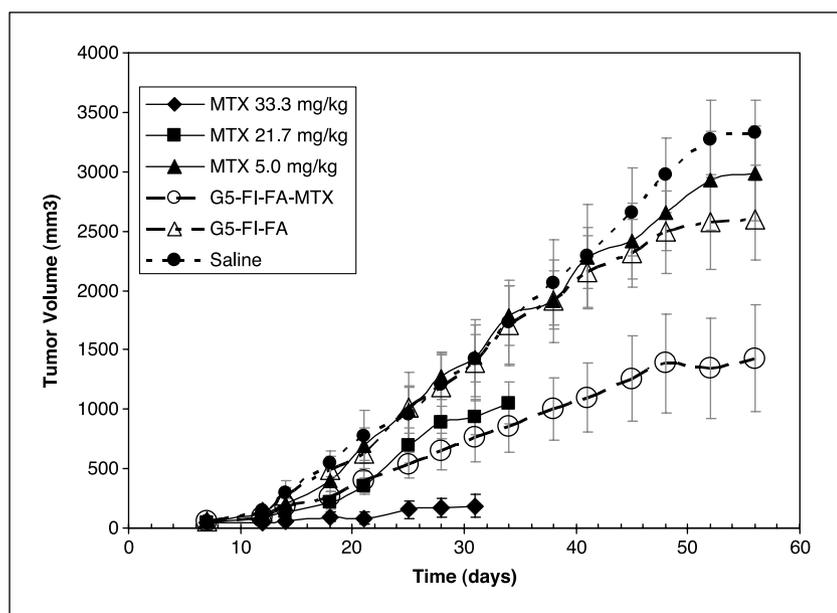


**Figure 3.** Tumor growth in SCID mice bearing KB xenografts during treatment with G5-FI-FA-MTX conjugate and free methotrexate (*MTX*). Tumor volume (mm$^3$) was calculated using the formula for a standard volume of an ellipsoid. The dose of the conjugate (55.0 mg/kg) equivalent to the lowest dose of free methotrexate (5.0 mg/kg) is as effective in tumor growth delay as the intermediate dose of free methotrexate (21.7 mg/kg). The lowest dose of free methotrexate (5.0 mg/kg) does not inhibit the tumor growth. During 15 biweekly injections (56 days) of the experiment, the highest dose of methotrexate (33.3 mg/kg) affected ~30% of the mice's body weight and was lethal (LD$_{50}$) at 32 days. The intermediate dose of free methotrexate (21.7 mg/kg) was lethal (LD$_{50}$) at 39 days, affecting ~30% of animal body weight. The remaining dose of free methotrexate (5.0 mg/kg) and all of the doses of the conjugates and control treatments were not toxic. *Points,* mean from five mice; *bars,* SE.

**Figure 4.** Survival rate of SCID mice bearing KB tumors. During 99 days of trial, mice received biweekly i.v. injections. Delivery of targeted conjugate with a fluorescent tag (G5-FI-FA-MTX) was compared with targeted conjugate without fluorescence (G5-FA-MTX), nontargeted conjugate (G5-FI-MTX), free methotrexate (*MTX*), conjugate without the drug (G5-FI-FA), and carrier control (saline). The drug in the nanoparticle was delivered in equimolar concentrations of free methotrexate. The dose of conjugate was calculated based on the total number of methotrexate molecules in the conjugate. The average total doses equivalent to methotrexate delivered to mice with G5-FI-FA-MTX, G5-FA-MTX, and G5-FI-MTX were 6.9, 7.2, and 5.0 mg/kg, respectively. The total dose of free methotrexate was 5.2 mg/kg. The final cumulative doses of the drug were not identical due to the different survival rates in the treated groups of mice. There were eight mice each in the methotrexate (*red*), G5-FI-MTX (*yellow*), G5-FA-MTX (*magenta*), and G5-FI-FA-MTX (*orange*) groups and seven mice in the saline (*blue*), and G5-FI-FA (*green*) control groups.
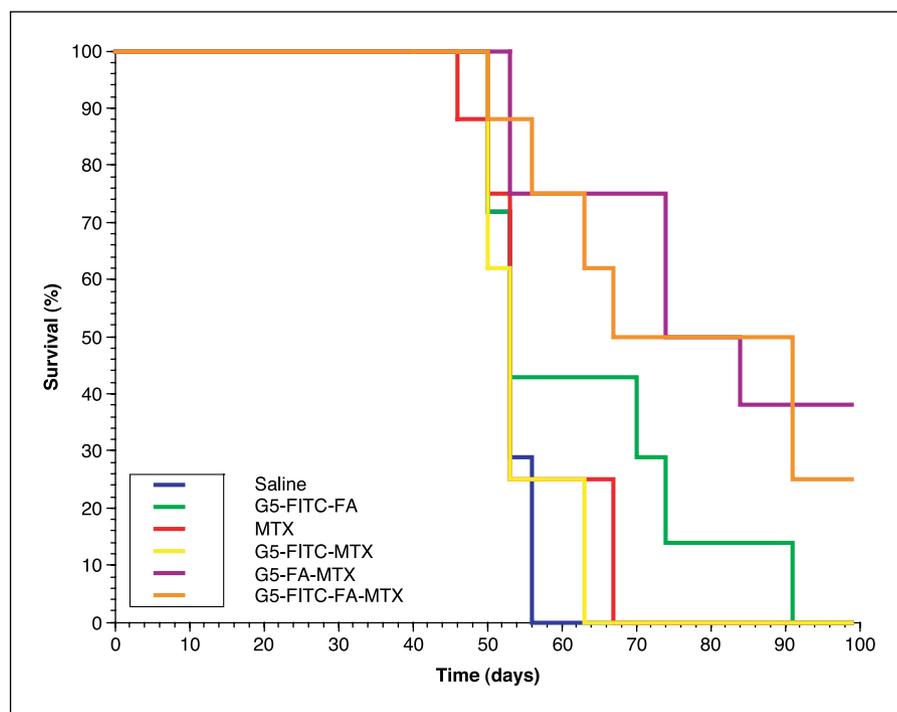
Confocal microscopy images show that labeled dendrimer conjugate is present within the cytosol of targeted cells (Fig. 2*D*). This is consistent with our *in vitro* binding and internalization studies of the multifunctional dendrimer conjugate (35). It also raises the possibility of releasing the drug within the targeted cells due to endosomal disruption of the acid-labile drug linker and provides additional specificity for the therapeutic. Internalization coupled with a high cytosolic concentration of the drug provides the possibility of overcoming drug nonresponsiveness due to the action of membrane P-glycoprotein in resistant tumor cells (36). Also of interest was that the antitumor activity of the targeting polymer therapeutic was equal whether it carried fluorescein (FITC; Fig. 4). This suggests that the four chemically distinct moieties on the conjugate, folic acid, fluorescent dye, radiolabel, and methotrexate, function independently. It raises hopes that other combinations of targeting and drug molecules as well as contrast agents for imaging can work independently when placed on the surface of the dendrimer.

We have achieved significant improvements in the therapeutic index of a targeted polymer-drug conjugate over a free drug, and this could have occurred from both a decrease in toxicity and an increase in drug effectiveness. Methotrexate conjugated to the dendrimer had significantly lower toxicity and 10-fold higher efficacy compared with free methotrexate at an equal cumulative dose (Fig. 3). We could also deliver higher dose of methotrexate on the conjugate compared with the free drug due to the longer survival of mice receiving the therapeutic nanoparticle (Fig. 4). However, the optimal dose of targeted drug has not been definitively established because no toxic dose of drug conjugate could be determined from either gross clinical evaluation or histopathology. Therefore, further studies with higher concentrations of dendrimer-targeted drugs are warranted.

Finally, these studies also document that this platform has the ability to deliver molecules to the interior of cancer cells, which may provide opportunities for therapies like genetic materials that must enter tumor cells to function. Although studies need to be conducted to address these approaches, there is the potential for a broad range of new therapeutic applications using this system.

## Acknowledgments

## References

1. Leamon CP, Reddy JA. Folate-targeted chemotherapy. Adv Drug Deliv Rev 2004;56:1127–41.
2. Weitman SD, Weinberg AG, Coney LR, Zurawski VR, Jennings DS, Kamen BA. Cellular localization of the folate receptor: potential role in drug toxicity and folate homeostasis. Cancer Res 1992;52:6708–11.
3. Campbell IG, Jones TA, Foulkes WD, Trowsdale J. Folate-binding protein is a marker for ovarian cancer. Cancer Res 1991;51:5329–38.
4. Weitman SD, Lark RH, Coney LR, et al. Distribution of the folate receptor GP38 in normal and malignant cell lines and tissues. Cancer Res 1992;52:3396–401.
5. Ross JF, Chaudhuri PK, Ratnam M. Differential regulation of folate receptor isoforms in normal and malignant tissues *in vivo* and in established cell lines. Physiologic and clinical implications. Cancer 1994;73:2432–43.
6. Antony AC, Kane MA, Portillo RM, Elwood PC, Kolhouse JF. Studies of the role of a particulate folate-binding protein in the uptake of 5-methyltetrahydrofolate by cultured human KB cells. J Biol Chem 1985;260:14911–7.
7. Lee RJ, Low PS. Folate-mediated tumor cell targeting of liposome-entrapped doxorubicin *in vitro*. Biochim Biophys Acta 1995;1233:134–44.
8. Wang S, Lee RJ, Cauchon G, Gorenstein DG, Low PS.

Delivery of antisense oligodeoxyribonucleotides against the human epidermal growth factor receptor into cultured KB cells with liposomes conjugated to folate via polyethylene glycol. Proc Natl Acad Sci U S A 1995; 92:3318–22.

9. Leamon CP, Low PS. Selective targeting of malignant cells with cytotoxin-folate conjugates. J Drug Target 1994;2:101–12.

10. Rund LA, Cho BK, Manning TC, Holler PD, Roy EJ, Kranz DM. Bispecific agents target endogenous murine T cells against human tumor xenografts. Int J Cancer 1999;83:141–9.

11. Cho BK, Roy EJ, Patrick TA, Kranz DM. Single-chain Fv/folate conjugates mediate efficient lysis of folate-receptor-positive tumor cells. Bioconjug Chem 1997;8: 338–46.

12. Kranz DM, Patrick TA, Brigle KE, Spinella MJ, Roy EJ. Conjugates of folate and anti-T-cell-receptor antibodies specifically target folate-receptor-positive tumor cells for lysis. Proc Natl Acad Sci U S A 1995;92:9057–61.

13. Roberts JC, Bhalgat MK, Zera RT. Preliminary biological evaluation of polyamidoamine (PAMAM) Starburst dendrimers. J Biomed Mater Res 1996;30:53–65.

14. Bielinska A, Kukowska-Latallo JF, Johnson J, Tomalia DA, Baker JR Jr. Regulation of *in vitro* gene expression using antisense oligonucleotides or antisense expression plasmids transfected using starburst PAMAM dendrimers. Nucleic Acids Res 1996;24:2176–82.

15. Kukowska-Latallo JF, Bielinska AU, Johnson J, Spindler R, Tomalia DA, Baker JR Jr. Efficient transfer of genetic material into mammalian cells using Starburst polyamidoamine dendrimers. Proc Natl Acad Sci U S A 1996;93:4897–902.

16. Malik N, Evagorou EG, Duncan R. Dendrimer-platinate: a novel approach to cancer chemotherapy. Anticancer Drugs 1999;10:767–76.

17. Wiener EC, Konda S, Shadron A, Brechbiel M, Gansow O. Targeting dendrimer-chelates to tumors and tumor cells expressing the high-affinity folate receptor. Invest Radiol 1997;32:748–54.

18. Malik N, Wiwattanapatapee R, Klopsch R, et al. Dendrimers: relationship between structure and biocompatibility *in vitro*, and preliminary studies on the biodistribution of $^{125}$I-labelled polyamidoamine dendrimers *in vivo*. J Control Release 2000;65:133–48.

19. Delong R, Stephenson K, Loftus T, et al. Characterization of complexes of oligonucleotides with polyamidoamine starburst dendrimers and effects on intracellular delivery. J Pharm Sci 1997;86:762–4.

20. Quintana A, Raczka E, Piehler L, et al. Design and function of a dendrimer-based therapeutic nanodevice targeted to tumor cells through the folate receptor. Pharm Res 2002;19:1310–6.

21. Nigavekar SS, Sung LY, Llanes M, et al. $^{3}$H dendrimer nanoparticle organ/tumor distribution. Pharm Res 2004; 21:476–83.

22. Majoros I, Keszler B, Woehler S, Bull T, Baker J. Acetylation of poly(amidoamine) dendrimers. Macromolecules 2003;36:5526–9.

23. Wilbur DS, Pathare PM, Hamlin DK, Buhler KR, Vessella RL. Biotin reagents for antibody pretargeting. 3. Synthesis, radioiodination, and evaluation of biotinylated starburst dendrimers. Bioconjug Chem 1998;9:813–25.

24. Turek JJ, Leamon CP, Low PS. Endocytosis of folate-protein conjugates: ultrastructural localization in KB cells. J Cell Sci 1993;106:423–30.

25. Mathias CJ, Wang S, Waters DJ, Turek JJ, Low PS, Green MA. Indium-111-DTPA-folate as a potential folate-receptor-targeted radiopharmaceutical. J Nucl Med 1998;39:1579–85.

26. Belz S, Nau H. Determination of folate patterns in mouse plasma, erythrocytes, and embryos by HPLC coupled with a microbiological assay. Anal Biochem 1998;265:157–66.

27. Nelson BC, Pfeiffer CM, Margolis SA, Nelson CP. Solid-phase extraction-electrospray ionization mass spectrometry for the quantification of folate in human plasma or serum. Anal Biochem 2004;325:41–51.

28. Thomas TP, Myaing MT, Ye JY, et al. Detection and analysis of tumor fluorescence using a two-photon optical fiber probe. Biophys J 2004;86:3959–65.

29. Griffin JL, Shockcor JP. Metabolic profiles of cancer cells. Nat Rev Cancer 2004;4:551–61.

30. Green MC, Murray JL, Hortobagyi GN. Monoclonal antibody therapy for solid tumors. Cancer Treat Rev 2000;26:269–86.

31. Davis TA, White CA, Grillo-Lopez AJ, et al. Single-agent monoclonal antibody efficacy in bulky non-Hodgkin's lymphoma: results of a phase II trial of rituximab. J Clin Oncol 1999;17:1851–7.

32. Sapra P, Allen TM. Internalizing antibodies are necessary for improved therapeutic efficacy of antibody-targeted liposomal drugs. Cancer Res 2002;62:7190–4.

33. Park JW, Hong K, Kirpotin DB, et al. Anti-HER2 immunoliposomes: enhanced efficacy attributable to targeted delivery. Clin Cancer Res 2002;8:1172–81.

34. Maeda H, Wu J, Sawa T, Matsumura Y, Hori K. Tumor vascular permeability and the EPR effect in macromolecular therapeutics: a review. J Control Release 2000;65: 271–84.

35. Thomas TP, Majoros IJ, Kotlyar A, et al. Targeting and inhibition of cell growth by an engineered dendritic nanodevice. J Med Chem. In press 2005.

36. Krishna R, Mayer LD. Multidrug resistance (MDR) in cancer. Mechanisms, reversal using modulators of MDR and the role of MDR modulators in influencing the pharmacokinetics of anticancer drugs. Eur J Pharm Sci 2000;11:265–83.

**AACR** American Association for Cancer Research

# Nanoparticle Targeting of Anticancer Drug Improves Therapeutic Response in Animal Model of Human Epithelial Cancer

Jolanta F. Kukowska-Latallo, Kimberly A. Candido, Zhengyi Cao, et al.

| | |
|---|---|
| **Updated version** | Access the most recent version of this article at:<br>http://cancerres.aacrjournals.org/content/65/12/5317 |

| | |
|---|---|
| **Cited articles** | This article cites 35 articles, 12 of which you can access for free at:<br>http://cancerres.aacrjournals.org/content/65/12/5317.full#ref-list-1 |
| **Citing articles** | This article has been cited by 11 HighWire-hosted articles. Access the articles at:<br>http://cancerres.aacrjournals.org/content/65/12/5317.full#related-urls |

| | |
|---|---|
| **E-mail alerts** | Sign up to receive free email-alerts related to this article or journal. |
| **Reprints and Subscriptions** | To order reprints of this article or to subscribe to the journal, contact the AACR Publications Department at pubs@aacr.org. |
| **Permissions** | To request permission to re-use all or part of this article, use this link<br>http://cancerres.aacrjournals.org/content/65/12/5317.<br>Click on "Request Permissions" which will take you to the Copyright Clearance Center's (CCC)<br>Rightslink site. |